HYDRAULIC CLARI-FLOCCULATION FOR CHEMICALLY ENHANCED PRIMARY TREATMENT OF SEWAGE

Mohamed Ayoub[1], Ahmed El-Morsy[1], and Ibrahim Gar Al-Alm Rashed[2]
[1]Public Works Engineering Department, Faculty of Engineering, Tanta University, Tanta
[2]Faculty of Engineering, Mansoura University & Dean of the Higher Institute for Engineering and Technology, New Damietta, Egypt

ABSTRACT

Chemical pre-precipitation becomes one of the best options of chemical treatment of sewage. In the present study, chemical pre-precipitation was processed via swirl flow hydraulic clari-flocculators, which were investigated using the steady state analysis versus the simulation using of computational fluid dynamics (CFD) software for the optimal model configuration, as well as the design equations of swirl flow hydraulic clari-flocculators were derived in the present study. From the obtained results, it can be demonstrated that up flow flocculation relatively improves regularity of tapering of velocity gradient rather than down flow flocculation. Furthermore, gravitational acceleration helps to form supplementary tapering in values of velocity gradients for up flow flocculation in contrast to down flow flocculation where gravitational acceleration negatively affects on tapering of velocity gradient.

Keywords: Clari-flocculators, Computational fluid dynamics (CFD), Hydraulic flocculation, Sewage treatment, Swirl flow

1 INTRODUCTION

Chemical precipitation was evaluated to enhance the primary treatment of sewage by coagulation, flocculation, and sedimentation processes (Younis et al. [1], Rashed at al. [2]); it was observed that reasonable removals of pollutants have been attained with 10 minutes of slow mixing followed by 20 minutes of settling time rather than 2 hours at least in the conventional primary treatment process [i.e. reached above 90%, and 70% for total suspended solids (TSS), and biological oxygen demand (BOD_5), respectively]. This creates research challenges for upgrading of the existing conventional sewage treatment plants on the same occupied area, or more precisely, redesign of the existing treatment units to accommodate higher design discharges without reduction in effluent quality (Younis et al.,1998), and (Rashed at al.,1997); considering that it is necessary to restructure the conventional primary sedimentation tanks to be swirl flow hydraulic clari-flocculators, where partitioning into flocculation zone achieved by swirl flow, and gravity sedimentation zone in the same tank, as well be seen in the present study.

Hydraulic clari-flocculators have been recently investigated in the field of water treatment through hydraulic mixing in a single basin, where combines flocculation and sedimentation (Engelhardt, 2010), and (El-Bassuoni et al., 2005). Moreover, hydraulic clari-flocculators provide excellent solids contact, accelerated floc formation and exceptional solids capture. This concept was applied in different designs (e.g. Spiracone™ by Siemens, and Claricone® by CB& I, Inc.) (Engelhardt [3]).On the other hand, (El-Bassuoni et al.,2005) presented an innovative system for water clarification that depends on hydraulic clari-flocculation by in-line mixing and it merges flocculation and clarification processes; this system reduced about 25% of the detention time compared with low cost technology used in the potable water treatment.

Gravity sedimentation has different applications in the primary treatment of sewage; it occurs in grit removal chambers as well as primary clarifiers, which remove about 65% of TSS, and about 35% of BOD_5. The settling rate was controlled by Stoke's law (Richardson et al., 2002) and (Crittenden et al., 2005), whereas the centrifugal force is utilized to enhance solids separation in different applications

(McCable et al., 1993), (Chiang, 2005), (Davailles et al., 2012), (Xu et al., 2009), (Brennan et al., 2009), and (Yuan Hsu et al., 2011).

The use of computational fluid dynamics (CFD) within water and wastewater treatment has only begun recently. However, interest and experience in this field are both growing apace, now CFD has been successfully used in analysis of water and wastewater treatment units (e.g. raw water reservoirs, flocculation tanks, and sedimentation tanks). Using CFD, it is possible to predict the information necessary to design, optimize or retrofit various treatment processes. Further advantages include reduced lead- in times and costs for new designs, the ability to examine the behavior of systems at the limit or beyond design capacity, and the ability to study large systems where controlled experiments at full- scale would be difficult, if not impossible to perform (Davailles et al., 2012), (Anderson, 1995), and (Bridgeman et al., 2009).

The undertaken work is devoted to apply the steady state analysis versus the use of the numerical simulation via CFD software for the optimal model configuration of swirl flow hydraulic clari-flocculators, which can be used to improve the quality and quantity of the primary treatment of sewage after restructuring of the conventional primary sedimentation tanks; also, the present study aims to derive the design equations of swirl flow hydraulic clari-flocculators.

2 METHOD

2.1 Models of swirl flow hydraulic flocculator

Figure (1) represents two different models of hydraulic flocculators using swirl flow; in figure (1-a), the tangential inlet was positioned at the bottom of the tank (nearly at radius of r_1) to generate a swirl flow in the conical tank in upward direction; whereas, in figure (1-b), the tangential inlet was positioned at the top of the tank to generate a swirl flow in the flocculation zone in downward direction. Velocity gradient (G-value), and angular velocity (ω) can be started at the level of the tangential inlet, subsequently they were tapered regularly even up to minimum value at the end of the flocculation zone.

Where:

- G_{12}= mean velocity gradient between radiuses r_1,and r_2 (s^{-1}),
- ω_{12}= mean angular velocity between radiuses r_1,and r_2 (s^{-1}),
- r_1 = radius of the tank at the position of the tangential inlet (m), and
- r_2= radius of the tank at the end of the flocculation zone (m).

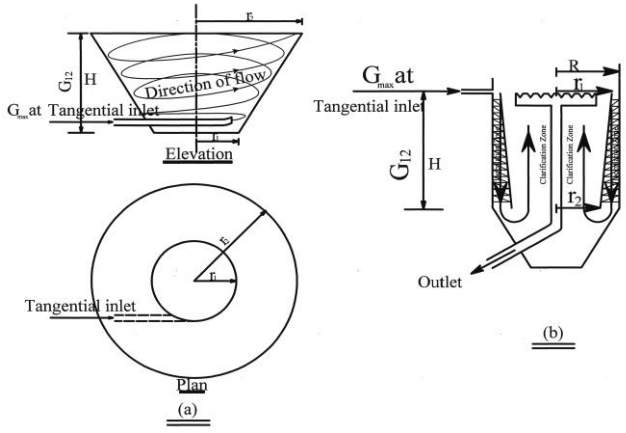

Figure 1: (a) Swirl flow hydraulic flocculator model (up flow model), (b) Swirl flow hydraulic flocculator model (down flow model) (El-Bassuoni et al., 2005)

2.2 Model development of swirl flow hydraulic clari-flocculator

In the present study, prototypes of swirl flow hydraulic clari-flocculator as shown in figures (2-b),and (2-c) can be developed as modifications of the conventional primary sedimentation tank as shown in figure (2-a) (Metcalf & Eddy, 2003), where flocculation and sedimentation processes can be amalgamated. In addition, the tangential inlet facilitates swirling flow and hydraulic mixing to generate a tapered velocity gradient from its level to the end of the flocculation zone (Engelhardt, 2010). The primary sedimentation tank shown in figure (2-a), was designed to treat 5000 m^3/d of de-gritted raw sewage in 2 hours of retention time with surface loading rate of 30 m^3/m^2/d to remove about 35% of BOD_5, and 65% of TSS (Metcalf & Eddy, 2003). Restructuring of the conventional primary sedimentation tank aims to double the design discharge (i.e. to be 10000 m^3/d) certainly with retention time of 1 hour (20 minutes for flocculation +40 minutes for sedimentation); i.e. adequate retention time to remove at least 65% of BOD_5, and 85% of TSS, according to references (Younis et al., 1998), (Rashed at al., 1997), and (Rashed et al.,2013).Moreover, Flow directions through flocculation zones were, up flow for prototype (1) in figure (2-b), and down flow for prototype (2) in figure (2-c) (Engelhardt, 2010), and (El-Bassuoni et al., 2005).Finally, average velocity gradient (G-value) was about 30 s^{-1} in the flocculation zones for prototypes (1,2).

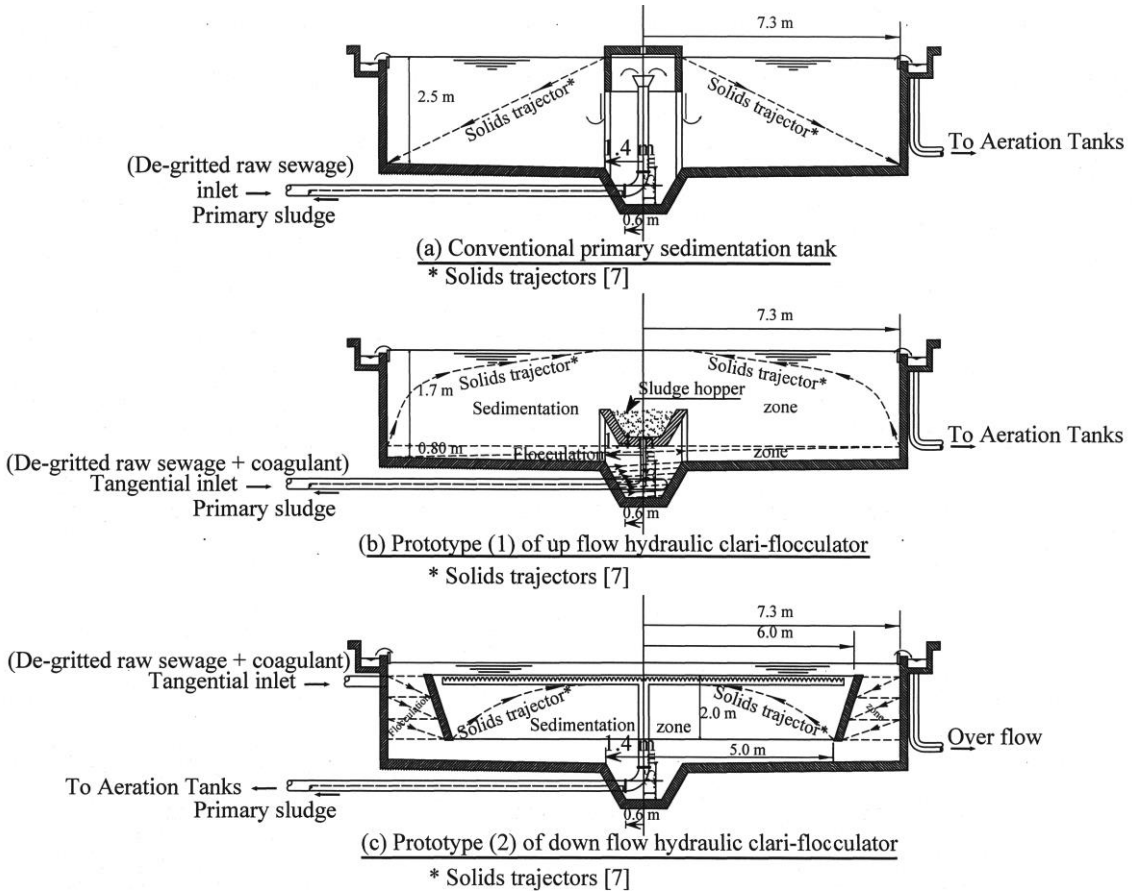

Figure 2: (a) Conventional primary sedimentation tank, (b) Prototype (1) of up flow hydraulic clari-flocculator (Engelhardt, 2010), (c) Prototype (2) of down flow hydraulic clari-flocculator (El-Bassuoni et al., 2005)

2.3 CFD software

Model development and simulation were based on commercial CFD software (Fluent 6.3), and meshing software (Gambit 2.4) (Fluent Inc., NH, USA). Fluent 6.3, which is a finite volume code was used in hydrodynamics and mass transfer computations, while Gambit 2.4 provides complete mesh flexibility in solving flow problems as well as boundary conditions may be determined by Gambit 2.4 software.

2.4 CFD modeling

The RNG k-ε model is the most suitable model for simulation of swirl flow hydraulic clari-flocculator; it provides an option to account for the effects of swirling by modifying the turbulence viscosity appropriately. Moreover, RNG k-ε model is suitable to handle low Reynold's number and near wall flows which occurred in sedimentation tanks (Xu et al.,2009), and (Bridgeman et al.,2009).

3 RESULTS AND DISCUSSION

3.1 Investigation of hydraulic flocculation using tangential inlet to form a swirl flow

The basic equation for the velocity gradient (G- value) and the power dissipated into water (P) are (Crittenden et al., 2005), and (Metcalf & Eddy, 2003):

$$P = \mu V G^2 = \frac{1}{2} C_d \rho_w A_c v_t^3$$

Where:

- P= average power dissipated into water (watt),
- V= volume of the flocculation tank (m^3),
- μ= absolute viscosity of the water (Kg.m/s),
- G= average velocity gradient (s^{-1}),
- A_c= contact area (m^2),
- ρ_w= water density (Kg/m^3),
- C_d= drag coefficient of water, and
- v_t= linear tangential velocity of the mixing (m/s) (constant through flocculation zone).

Figures (3-a), and (3-b) represent models of hydraulic flocculators using swirl flow; the design equation of a swirl flow hydraulic flocculators for each model can be derived as the following:

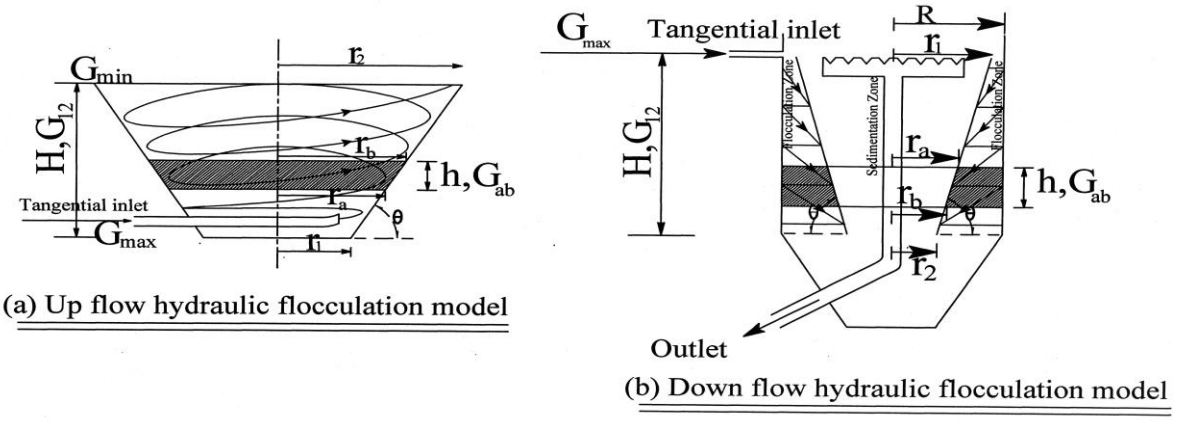

Figure 3: (a) Up flow hydraulic flocculation model, (b) Down flow hydraulic flocculation model (El-Bassuoni et al., 2005)

From the geometry of the hatched volume element for up flow model in figure (3-a),

$$A_c = \pi h(r_a + r_b)$$

$$, v_t = \omega_{ab} r = \omega_{ab}\left(\frac{r_a + r_b}{2}\right)$$

$$, V = \frac{\pi h}{3}(r_a^2 + r_b^2 + r_a r_b)$$

$$\because P = \mu V G^{2} = \frac{1}{2} C_d \rho_w A v_t^3$$

$$\therefore \mu * \frac{\pi h}{3}(r_a^2 + r_b^2 + r_a r_b) G_{ab}^{2} = \frac{1}{2} C_d \rho_w \pi h (r_a + r_b) \omega_{ab}^3 (\frac{r_a + r_b}{2})^3$$

Hence, tapering of velocity gradient for up flow model can be derived from the following equation:

$$\therefore G_{ab}^{2} = \frac{3 C_d \rho_w}{16 \mu} * \frac{(r_a + r_b)^4 \omega_{ab}^{3}}{(r_a^2 + r_b^2 + r_a r_b)} \quad (1)$$

From figure (3-a), $r_b = r_a + \frac{h}{\tan\theta}$ substitute in equation (1),

$$\therefore G_{ab}^{2} = \frac{3 C_d \rho_w}{16 \mu} * \frac{(2r_a + \frac{h}{\tan\theta})^4 \omega_{ab}^{3}}{(3r_a^2 + \frac{3 r_a h}{\tan\theta} + \frac{h^2}{\tan^2\theta})}$$

Where:

- G_{ab}= average velocity gradient between radiuses r_a, and r_b (s^{-1}),
- ω_{ab}= average angular velocity between radiuses r_a, and r_b (s^{-1}),
- h= height of the volume element in the flocculation zone (m), and
- θ= inclination angle of the cone in the flocculation zone.

On the other hand, from the geometry of the hatched volume element for down flow model in figure (3-b),

$$A_c = \pi h (r_a + r_b) + 2\pi R h = \pi h [2R + (r_a + r_b)]$$

$$, v_t = \omega_{ab} [\frac{2R - (r_a + r_b)}{2}]$$

$$, V = \pi R^2 h - \frac{\pi h}{3}(r_a^2 + r_b^2 + r_a r_b) = \pi h [R^2 - \frac{1}{3}(r_a^2 + r_b^2 + r_a r_b)]$$

$$\because P = \mu V G^{2} = \frac{1}{2} C_d \rho_w A v_t^3$$

$$\therefore \mu * \pi h [R^2 - \frac{1}{3}(r_a^2 + r_b^2 + r_a r_b)] G_{ab}^{2} = \frac{1}{2} C_d \rho_w \pi h [2R + (r_a + r_b)] v_t^3$$

Tapering of velocity gradient for up flow model can be derived from the following equations:

$$\therefore G_{ab}^{2} = \frac{C_d \rho_w}{2 \mu} * \frac{[2R + (r_a + r_b)]}{[R^2 - \frac{1}{3}(r_a^2 + r_b^2 + r_a r_b)]} * v_t^3 \quad (2)$$

$$\text{or}, G_{ab}^{2} = \frac{C_d \rho_w}{16 \mu} * \frac{[2R + (r_a + r_b)][2R - (r_a + r_b)]^3}{[R^2 - \frac{1}{3}(r_a^2 + r_b^2 + r_a r_b)]} * \omega_{ab}^3 \quad (3)$$

From figure (3-b), $r_b = r_a - \frac{h}{\tan\theta}$ substitute in equation (2),

$$\therefore G_{ab}{}^2 = \frac{C_d \rho_w}{2\mu} * \frac{(2R + 2r_a - \frac{h}{\tan\theta})}{[R^2 - \frac{1}{3}(3r_a^2 + \frac{3r_a h}{\tan\theta} + \frac{h^2}{\tan^2\theta})]} * v_t^3$$

Where:

- G_{ab}= average velocity gradient between radiuses r_a, and r_b (s^{-1}),
- ω_{ab}= average angular velocity between radiuses r_a, and r_b (s^{-1}),
- h= height of the volume element in the flocculation zone (m),
- θ= inclination angle of the cone in the flocculation zone, and
- R= radius of the clari-flocculator (m).

3.2 Tapering of velocity gradient in prototype (1)

Prototype (1) was evaluated according to tapering of velocity gradients using the derived design equation (1) versus CFD simulation via (Fluent 6.3, and Gambit 2.4) software. Figure (4-a) shows position of the tangential inlet and limit of the flocculation zone in prototype (1). Moreover, figure (4-b) represents the tapering of (G-values) through depth of clari-flocculator resulted from CFD simulation and derived equation (1), neglecting effect of the gravitational acceleration. Third order polynomial regression was applied for analysis of tapering of (G-values) resulted from CFD simulation and equation (1); regression analysis was performed to clarify the convergence of (G-values) resulted from CFD simulation and equation (1) as shown in figure (4-b), where best fit equations were displayed [i.e. equations (I, II)]. It is noticed that (G-values) were tapered regularly through flocculation zone depth with rate of 39.5 s^{-1}/m depth [using CFD simulation] versus 32.5 s^{-1}/m depth [using equation (1)].

On the other hand, CFD simulation was processed considering the gravitational acceleration; (G-values) were relatively declined in comparison with neglecting effect of the gravitational acceleration. Hence, gravitational acceleration result noticeable differences in velocity gradient (ΔG) through depth of the flocculation zone (d); then, correction of velocity gradient (ΔG) can be determined using of dimensional analysis as follows:

$$\Delta G = G_g - G = f(g, d) = k g^a d^b$$

Where:

- ΔG = velocity gradient resulted from effect of the gravitational acceleration (s^{-1}),
- G_g= (G- values) with considering of the gravitational acceleration (s^{-1}),
- G= (G- values) with neglecting of the gravitational acceleration (s^{-1}),
- g= gravitational acceleration =9.81m/s^2,
- d= flocculation depth, measured from the tangential inlet level (m), and
- k= an empirical coefficient deduced in section (3.4).

The previous equation must be dimensionally homogenous; the exponents of each of the quantities must be the same on each side of the equation;

$$\therefore T^{-1} = (LT^{-2})^a (L)^b = (L)^{a+b} (T)^{-2a}$$

$$\therefore a = 0.5, b = -0.5$$

$$\therefore \Delta G = k\sqrt{\frac{g}{d}} \quad (4)$$

The corrected velocity gradient (G_g-values) can be determined by modifying equation (1) as follows:

$$(G_{ab})_g = \sqrt{\frac{3C_d\rho_w}{16\mu} * \frac{(r_a + r_b)^4 \omega_{ab}^{\ 3}}{(r_a^2 + r_b^2 + r_a r_b)}} + k\sqrt{\frac{g}{d}} \qquad (5)$$

In case of prototype (1), k= -1.9. As shown in figure (4-b), (G-values) were corrected using the modified design equation (5). Also, regression analysis was applied for the corrected values to clarify the convergence of (G- values) resulted from CFD simulation (considering gravitational acceleration), and derived equation (5) as shown in figure (4-b), where best fit equations were displayed [i.e. equations (III, IV)].

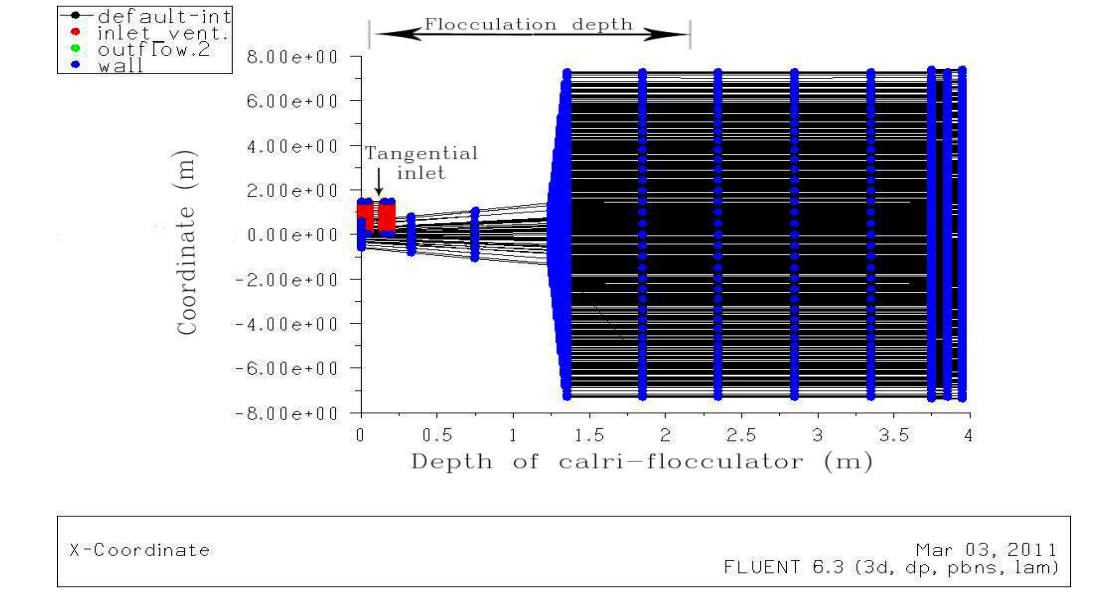

(a)

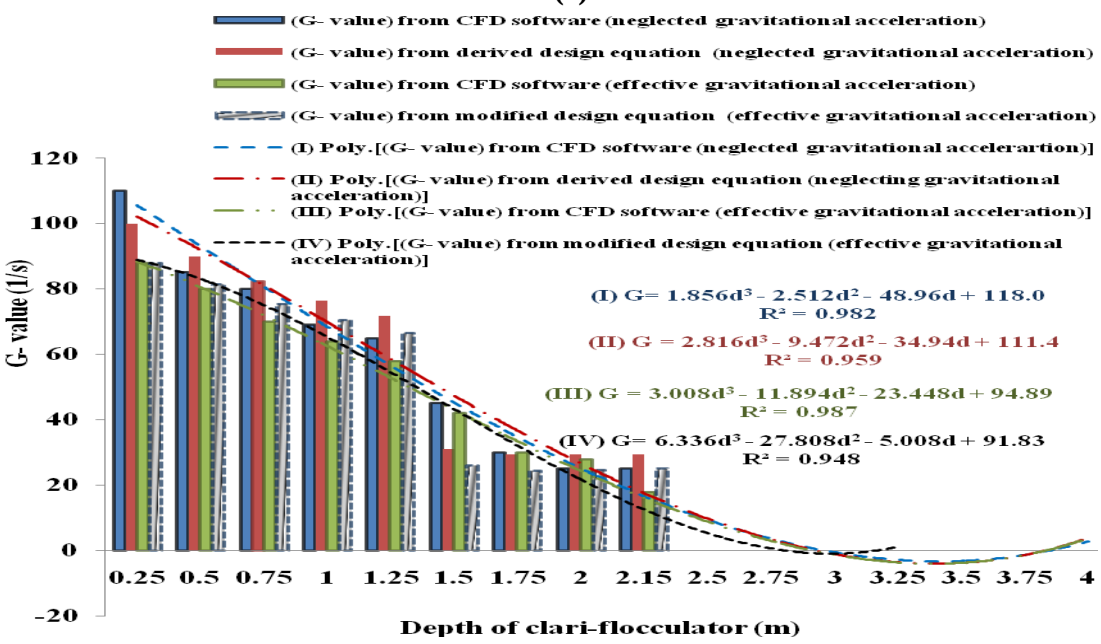

(b)

Figure 4: (a) Geometry of prototype (1), (b) (G-values) resulted from CFD simulation and derived design equations for prototype (1)

3.3 Tapering of velocity gradient in prototype (2)

Prototype (2) was evaluated according to tapering of velocity gradients using the derived design equations (2, 3) versus CFD simulation via (Fluent 6.3, and Gambit 2.4) software; Figure (5-a) shows position of the tangential inlet and limit of the flocculation zone in prototype (2). Moreover, figure (5-b) represents the tapering of (G-values) through depth of clari-flocculator resulted from CFD simulation and derived equations (2, 3), neglecting effect of the gravitational acceleration. Third order polynomial regression was applied for analysis of tapering of (G-values) resulted from CFD simulation and equation (3); regression analysis was performed to clarify the convergence of (G-values) resulted from CFD simulation and equation (3) as shown in figure (5-b), where best fit equations were displayed [i.e. equations (I, II)]. It is noticed that (G-values) were tapered through flocculation zone depth with relatively small rate of 9 s^{-1}/m depth [using CFD simulation] versus 3.9 s^{-1}/m depth [using equation (3)].

On the other hand, CFD simulation was processed considering the gravitational acceleration; (G-values) were relatively increased in comparison with neglecting effect of the gravitational acceleration. Hence, gravitational acceleration result noticeable differences in velocity gradient (ΔG) through depth of the flocculation zone (d); then, correction of velocity gradient (ΔG) can be determined using the previously derived equation (4):

$$\Delta G = k\sqrt{\frac{g}{d}} \tag{4}$$

The corrected velocity gradient (G_g-values) can be determined by modifying equation (3) as follows:

$$(G_{ab})_g = \sqrt{\frac{C_d \rho_w}{16\mu} * \frac{[2R + (r_a + r_b)][2R - (r_a + r_b)]^3}{[R^2 - \frac{1}{3}(r_a^2 + r_b^2 + r_a r_b)]} * \omega_{ab}^3} + k\sqrt{\frac{g}{d}} \tag{6}$$

In case of prototype (2), k= 3.4. As shown in figure (5-b), (G-values) were corrected using the modified design equation (6). Also, regression analysis was achieved for the corrected values to clarify the convergence of (G-values) resulted from CFD simulation (considering gravitational acceleration), and derived equation (6) as shown in figure (5-b), where best fit equations were displayed [i.e. equations (III, IV)].

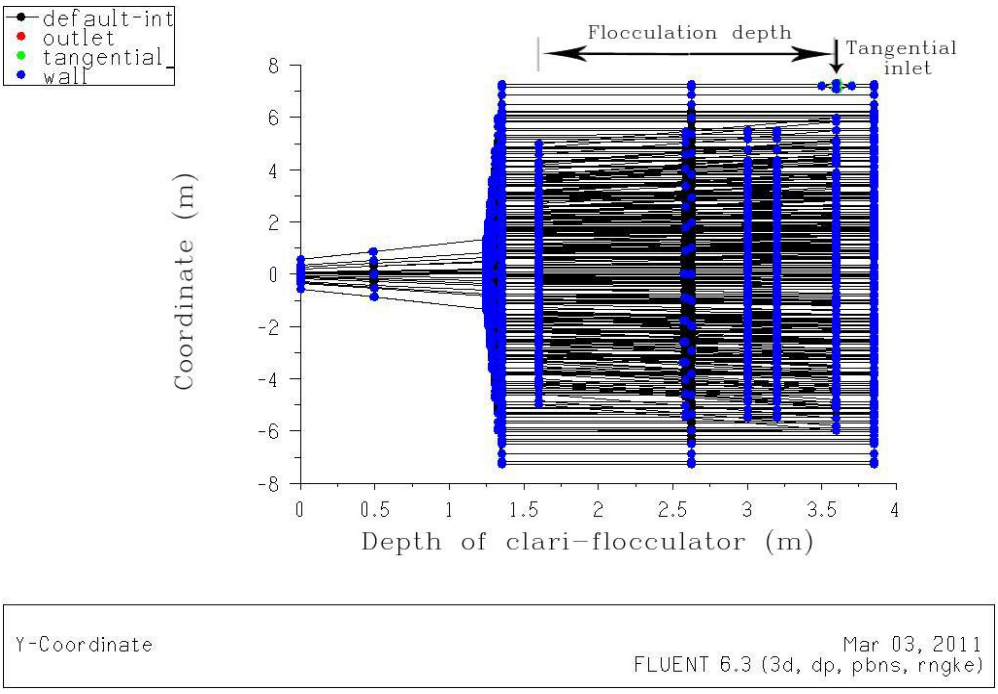

(a)

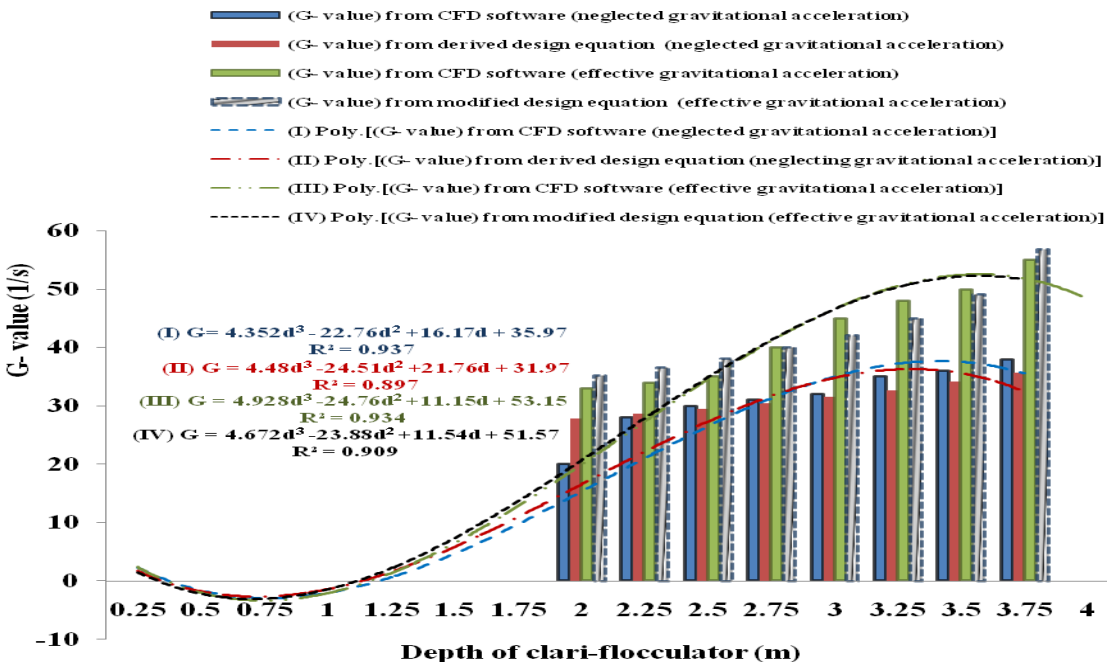

(b)

Figure 5: (a) Geometry of prototype (2), (b) (G-values) resulted from CFD simulation and derived design equations for prototype (2)

3.4 Estimation of velocity gradient resulting from the gravitational acceleration

Empirical coefficient (k) resulted from the dimensional analysis as explained in equation (4), can be deduced by comparing (G-values) resulted from CFD simulation in cases of neglecting and considering effect of the gravitational acceleration; CFD simulation was processed for different sizes and configurations of hydraulic clari-flocculators, which ranged between 5m to 40m in diameter. Consequently, a logarithmic regression was applied for the different results to predict the best fit equations as shown in figure (6), where the empirical coefficient (k) can be determined for the different types and dimensions of swirl flow hydraulic clari-flocculators.

From equations (5, and 6), the corrected velocity gradient (G_g-values) can be determined using the following equations:
For up flow flocculation,

$$(G_{ab})_g = \sqrt{\frac{3C_d\rho_w}{16\mu} * \frac{(r_a + r_b)^4 \omega_{ab}^{\ 3}}{(r_a^2 + r_b^2 + r_a r_b)}} - \sqrt{\frac{g}{d}}[1.39\ln(\frac{\phi}{5}) + 0.043] \quad (7)$$

For down flow flocculation,

$$(G_{ab})_g = \sqrt{\frac{C_d\rho_w}{16\mu} * \frac{[\phi + (r_a + r_b)][\phi - (r_a + r_b)]^3}{[\frac{\phi^2}{4} - \frac{1}{3}(r_a^2 + r_b^2 + r_a r_b)]} * \omega_{ab}^3} + \sqrt{\frac{g}{d}}[2.51\ln(\frac{\phi}{5}) + 0.072] \quad (8)$$

Where:

- $(G_{ab})_g$= average velocity gradient between radiuses r_a, and r_b ,considering the gravitational acceleration(s^{-1}),
- C_d= drag coefficient of water,
- ρ_w= water density (Kg/m^3),
- μ= absolute viscosity of the water (Kg.m/s),
- Φ= diameter of clari-flocculator (m),
- ω_{ab}= average angular velocity between radiuses r_a, and r_b (s^{-1}),
- g= gravitational acceleration =$9.81 m/s^2$, and
- d= flocculation depth, measured from the tangential inlet level (m).

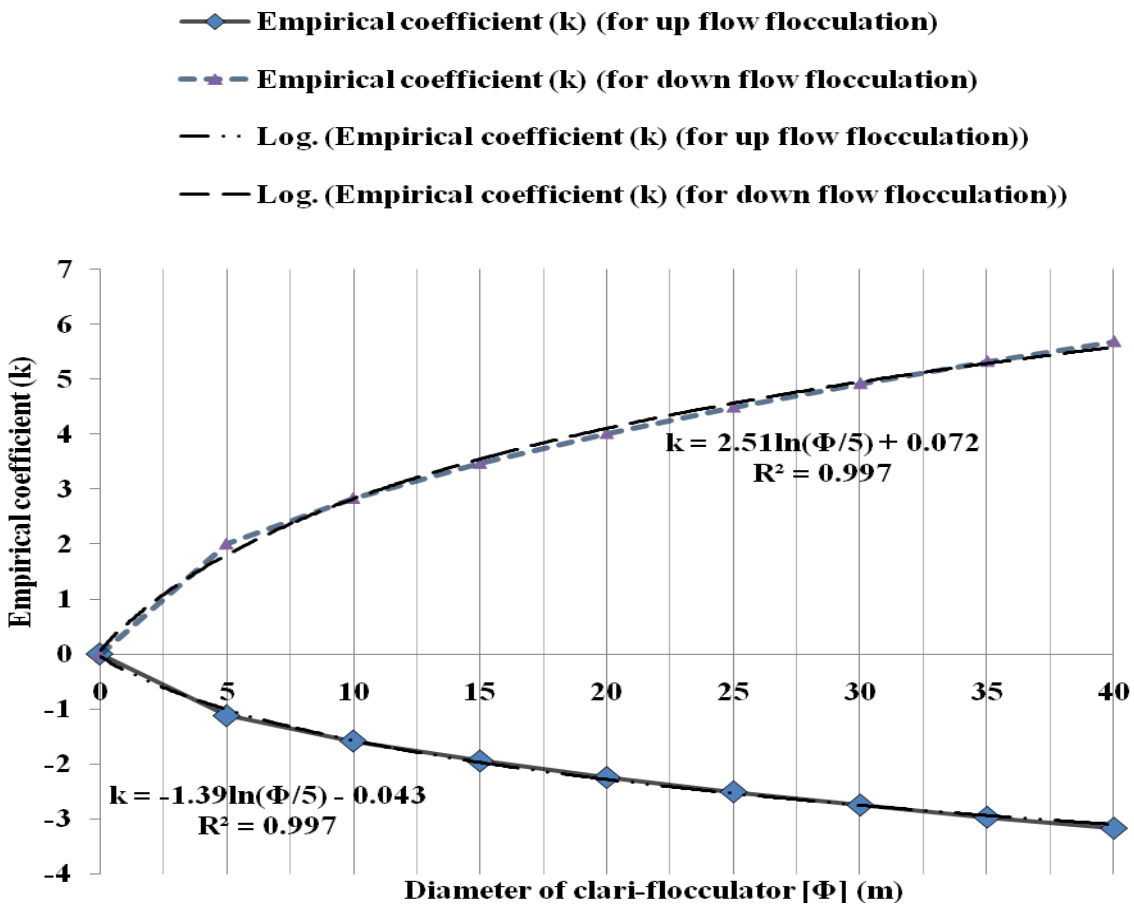

Figure 6: Empirical coefficient (k) for up flow and down flow flocculation

3.5 Evaluation of the different prototypes

From the previous results, it is noticed that (G-values) were tapered through flocculation depth with rate about 33.6 s^{-1}/m depth, from the different results of prototype (1); While, rate of tapering of (G-values) was about 8.7 s^{-1}/m depth, from the different results of prototype (2). This means that rate of tapering of (G-values) in upward swirl flow (1) roughly equal to 4 times its value in downward swirl flow, which indicates that gravitational acceleration relatively improves regularity of tapering of (G-values) for up flow flocculation, whereas it declines to some extent the tapering of (G-values) for down flow flocculation, where (G-values) seemed to be almost constant. Therefore, prototype (1) as a model of up flow hydraulic clari-flocculator is preferable as a modification of the conventional primary sedimentation tank to accommodate excess flow rate of sewage.

On the other hand, the barrier between the flocculation and clarification zones in the prototype (2) adds a comparative advantage compared with prototype (1) summarized in retaining of the formed flocs from cracking. In addition, downward swirl flow [prototype (2)] also features the upward swirl flow [prototype (1)] in the presence of sludge hopper at the bottom of the tank, which is poised to receive all sludge in the tank; while, the position of the sludge hopper over the flocculation zone in prototype (1) enables the small sediments to escape to the bottom of the tank, and it may be mixed with the raw sewage till increasing the concentration of the pollutants. Consequently, it may reduce the treatment efficiency. Therefore, prototype (2) is suitable for potable water purification to ensure the separation between flocculation and sedimentation processes, as well as prototype (2) may be appropriate for upgrading the sewage treatment plants designed without primary sedimentation (e.g. oxidation ditches system); while, prototype (1) is suitable for the enhancement of the primary

treatment of sewage, especially, in the already existing plants which contain primary sedimentation tanks.

4 CONCLUSIONS

The obtained results reveal the following conclusions:

- The tapering of velocity gradient is more regular in upward swirl flow rather than downward swirl flow.
- Gravitational acceleration relatively improves regularity of tapering of (G- values) for up flow flocculation, whereas it declines to some extent the tapering of (G-values) for down flow flocculation, where (G-values) seemed to be almost constant.
- The barrier between the flocculation and clarification zones in the prototype (2) adds a comparative advantage compared with prototype (1) summarized in retaining of the formed flocs from cracking.
- Downward swirl flow [prototype (2)] also features the upward swirl flow [prototype (1)] in the presence of sludge hopper at the bottom of the tank, which is poised to receive all sludge in the tank; while, the position of the sludge hopper over the flocculation zone in prototype (1) enables the small sediments to escape to the bottom of the tank, and it may be mixed with the raw sewage till increasing the concentration of the pollutants. Consequently, it may reduce the treatment efficiency. Therefore, prototype (2) is suitable for potable water purification to ensure the separation between flocculation and sedimentation processes, as well as prototype (2) may upgrade the sewage treatment plants designed without primary sedimentation (e.g. oxidation ditches system); while, prototype (1) is suitable for the enhancement of the primary treatment of sewage, especially, in the already existing plants which contains primary clarifiers.

REFERENCES

[1]. Anderson, J.D. (1995). *Computational Fluid Dynamics: The Basics with Applications*. Mechanical Engineering Series. Mc Graw- Hill International Editions. ISBN 0-07-113210-4

[2]. Brennan, M; Holtham, P; and Narasimha, M. (2009). CFD Modeling of Cyclone Separator: Validation against plant hydrodynamics performance. *7th International Conference on CFD in the Minerals and Process Industries*, CSIRO, Melbourne, Australia

[3]. Bridgeman, J; Jefferson, B; and Parson, S.A. (2009). Computational Fluid Dynamics Modeling of Flocculation in Water Treatment: A Review. *Engineering Applications of Computational Fluid Mechanics*. Vol. 3, No.2, pp.220-241

[4]. Chiang, S.H. (2005). *Solid- Liquid Separation*. CRC Press LLC.

[5]. Crittenden, J.C; Trussel,R.R; Hand, D.W. ; Howe, K.J; and Tchobanoglous, G.(2005) *Water Treatment Principles and Design*. second edition , Jhon Wiley and Sons Inc.

[6]. Davailles, A; Climent, E; and Bourgeois, F.(2012). Fundamental understanding of swirling flow pattern in hydrocyclones. *Separation and Purification Technology,* Vol.92. pp. 152-160. ISSN 1383-5866

[7]. El-Bassuoni, A.A; Rashed, I.G.; Al-Sarawy, A.A; and El-Halwany, M.M.(2005). A Novel Compact Coagulation-Flocculation-Sedimentation System. *9th International Water Technology Conference,* Sharm El-Sheikh, Egypt

[8]. Engelhardt, T.L. (2010). Coagulation, Flocculation and Clarification of Drinking Water. *Drinking water sector, Hach Company*

[9]. McCable, W.L; Smith, J.C; and Harriott, P. (1993). *Unit Operation of Chemical Engineering.* 5th edition. McGraw Hill

[10]. Metcalf & Eddy, Inc., George Tchobanoglous; Franklin L. Burton; and H. David Stensel. (2003). *Wastewater Engineering Treatment and Reuse*. 4th ed., Mc Graw-Hill

[11]. Rashed, I.G; Afify, H. A; Ahmed, A.E; and Ayoub, M. A. (2013). Optimization of chemical precipitation to improve the primary treatment of wastewater. *Journal of Desalination and Water Treatment*, USA. (In press)

[12]. Rashed, I.G; El-Komy, M. A; Al-Sarawy, A. A; and Al-Gamal, H. F, (1997). Chemical Treatment of Sewage. *the First Scientific Conference of the Egyptian Society for the Development of Fisheries Resources and Human Health*, El Arish, Egypt

[13]. Richardson, J.F; Harker, J.H; and Backhurst, J.R. (2002). *Chemical Engineering Series: Particle Technology and Separation Processes*. Volume (2). Butterworth- Heinemann, Oxford

[14]. Xu, Peng; Wu, Zhonghua; and Mujumdar, Aruns. (2009). Mathematical Modeling of Industrial Transport Processes. *National University of Singapore*

[15]. Younis, S.S; Al Mansi, N.M; and Fouad, S.H. (1998). Chemically assisted primary treatment of municipal wastewater. *Journal of Environmental Management and Health* p.p:209-214

[16]. Yuan Hsu, Chih; Jhih Wu, Syuan; and Ming Wu, Rome. (2011). Particles Separation and Tracks in Hydrocyclone. *Tamkang Journal of Science and Engineering*, Vol.14, No.1, pp. 65-70